PCCP

Cite this: *Phys. Chem. Chem. Phys.*, 2011, **13**, 20575–20583

www.rsc.org/pccp

PAPER

Size dependences of the diradical character and the second hyperpolarizabilities in dicyclopenta-fused acenes: relationships with their aromaticity/antiaromaticity

Shuto Motomura,[a] Masayoshi Nakano,*[a] Hitoshi Fukui,[a] Kyohei Yoneda,[a] Takashi Kubo,[b] Raphaël Carion[c] and Benoît Champagne*[c]

Received 15th March 2011, Accepted 2nd June 2011
DOI: 10.1039/c1cp20773c

Using long-range corrected density functional theory, the relationships between the electronic, magnetic, and nonlinear optical properties are drawn for two families of organic compounds, the dicyclopenta-fused acenes (DPAs) and the polyacenes (PAs), containing up to $N = 12$ fused rings. First, the longitudinal second hyperpolarizability (γ) of singlet DPAs is significantly enhanced with increasing system size, in comparison to PAs. This behavior is associated with an increase in the longitudinal spin polarization between the terminal five-membered rings of DPAs and is consistent with previous studies where γ is maximized for intermediate diradical character. The size dependence of the diradical character is also found to cause a hump in the γ/N evolution for singlet DPAs around $N = 8$. In fact, in the case of singlet PAs, the diradical characters y_0 and y_1, the various magnetic properties and the γ/N values vary monotonically with N, whereas for singlet DPAs, the shielding, the magnetizability, and the γ/N values exhibit extrema near $N = 8$ due to the appearance of transversal spin polarization in the middle six-membered rings in addition to the longitudinal spin polarization between the terminal five-membered rings. Moreover, it is shown that for singlet DPAs the longitudinal spin polarization (characterized by y_0) is associated with the antiaromaticity ($N \leq 3$) and the slight- or non-aromaticity ($N \geq 4$) of the terminal five-membered rings, whereas the appearance of transversal spin-polarization (characterized by y_1) is associated with the decrease in the aromaticity in the inner six-membered rings as shown for large PAs. Therefore, the exceptional behaviors in singlet DPAs for small N ($N < 9$) are caused by the increase in diradical character y_0 correlated with the anti-aromaticity or the slight-/non-aromaticity of terminal rings and the corresponding emergence of a global aromatic character. Such a relationship between the aromaticity/antiaromaticity and the diradical character is useful for designing real open-shell NLO molecules through the control of their diradical characters.

1. Introduction

There is a renewed interest in diradical and multiradical systems, owing to the remarkable electronic, optical, and magnetic properties they can exhibit, in addition to their specific chemical reactivity.[1] Part of this interest is certainly attributed to the new graphitic systems, graphenes, graphene nanoribbons, and graphene nanoflakes,[2–4] as well as to the ability of organic chemistry to tailor nanographenes in order to achieve specific properties.[5–7] Among their specific properties are low-energy excited states,[8,9] tailorable low-spin/high-spin gaps,[10,11] high-yield singlet fissions,[12] short intermolecular distances in the solid state,[13–15] and large two-photon absorptions.[16] Therefore experimentalists and theoreticians invest a lot in their molecular design and in the understanding of their properties. The topic of this paper thus aims at assessing the nonlinear optical and magnetic properties of some of these compounds and at deducing relationships between them.

Recently, we have theoretically revealed the strong diradical character dependence of the second hyperpolarizability γ [the third-order nonlinear optical (NLO) property at the molecular scale]:[17–23] open-shell singlet molecules with intermediate diradical characters exhibit larger γ values than closed-shell and pure open-shell molecules. This structure–property relationship has been exemplified by using a simple two-site model in a valence

[a] *Department of Materials Engineering Science, Graduate School of Engineering Science, Osaka University, Toyonaka, Osaka 560-8531, Japan. E-mail: mnaka@cheng.es.osaka-u.ac.jp*
[b] *Department of Chemistry, Graduate School of Science, Osaka University, Toyonaka, Osaka 560-0043, Japan*
[c] *Laboratoire de Chimie Théorique, Facultés Universitaires Notre-Dame de la Paix (FUNDP), rue de Bruxelles, 61, 5000 Namur, Belgium. E-mail: benoit.champagne@fundp.ac.be*

configuration interaction scheme[20] as well as by *ab initio* molecular orbital (MO) and density functional theory (DFT) calculations on various open-shell molecules, *e.g.*, *p*-quinodimethane models,[17,18] diphenalenyl radicals[19] and graphene nanoflakes.[21–23] On the basis of these results, we have proposed several guidelines for controlling γ *via* tuning the diradical characters through the modification of molecular structures and/or the introduction of relevant substituents.

On the other hand, as one of the chemical concepts associated with the open-shell character, aromaticity has been discussed on theoretical grounds by Kertesz *et al.*[24] So, in antiaromatic or weakly-aromatic molecules, the near-degenerate electronic states are likely to enhance their diradical characters because the diradical character is defined by the weight of the doubly excited configuration in the ground state.[25–31] It is therefore worthwhile to investigate the relationship between the aromaticity/antiaromaticity and γ through the diradical character for several aromatic and antiaromatic molecules.

In this paper, we investigate the size dependences of the diradical characters and γ values of one-dimensional model antiaromatic molecules, *i.e.*, dicyclopenta-fused acenes (DPAs), by using the long-range corrected spin-unrestricted density functional theory, LC-UBLYP, method.[32] For comparison, we also examine model aromatic molecules, *i.e.*, polyacenes (PAs), which differ from DPAs in their two terminal ring structures. The degree of aromaticity is evaluated by (i) the nucleus-independent chemical shifts (NICSs), the opposite of the isotropic shielding constant, NICS $= -1/3(\sigma_{xx} + \sigma_{yy} + \sigma_{zz})$,[33] at different key positions in the space around the molecule as well as under the form of 3D iso-chemical shielding surfaces (ICSS),[34,35] (ii) the out-of-plane diagonal element of the σ tensor, $-\sigma_{zz}$, which is expected to highlight the specific behavior of the π-electrons and then expected to give a better appreciation of the (anti)-aromaticity evolution than the NICS criterion,[34] and (iii) the magnetic susceptibility (χ), and particularly its anisotropy, $\Delta\chi = \chi_{zz} - 1/2(\chi_{xx} + \chi_{yy})$, which can be mostly associated with the delocalization of the π-electrons and therefore with the eventual diatropicity (paratropicity) of the aromatic (antiaromatic) systems.[36] From these results, we explain the differences of the second hyperpolarizabilities, their dependence on the size of the molecule, and their relationship with the diradical character between DPAs and PAs from the viewpoint of aromaticity and antiaromaticity. The present study will thus provide a novel guideline to control the diradical characters and γ values in open-shell singlet molecules based on their aromaticity/antiaromaticity.

2. Methodology

2.1. Model molecules and geometries

Fig. 1 shows the structures of DPA (a) and PA (b) ($2 \leq N \leq 12$), where N denotes the number of fused rings including the terminal five- or six-membered rings. The geometries of all systems in their singlet states were optimized by the spin-unrestricted (U) B3LYP/6-311G* method under the constraint of D_{2h} symmetry. Although it is well-known that pentalene, *i.e.*, DPA($N = 2$), does not belong to the D_{2h} symmetry,[24,37] and that the equilibrium symmetry of

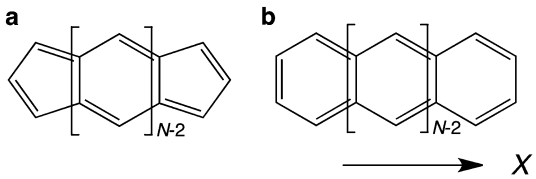

Fig. 1 Molecular structures of DPAs (a) and PAs (b), where N indicates the number of fused-ring units. The x coordinate axis is also shown.

s-indacene, *i.e.*, DPA($N = 3$), is in controversy,[24,38,39] we employed the D_{2h} symmetries for these molecules because such structural differences in pentalene and *s*-indacene, having small diradical characters, only give slight effects on the size dependences of γ in the intermediate and large diradical character regions tackled in this study.[40] Indeed, the difference in diradical characters between D_{2h} and C_{2h} symmetries for these molecules is small (less than $\sim$30%) for semi-quantitative discussion.

In addition, the UB3LYP/6-311G* solutions of PA($N = 2$–5) and DPA($N = 2$) coincide with the spin-restricted (R) B3LYP/6-311G* ones. This is consistent with the fact that molecules with relatively small diradical characters [calculated using the spin-unrestricted Hartree–Fock (UHF) method or DFT schemes with high amount of HF exchange] tend to have closed-shell solutions at the B3LYP level of approximation.[1,41]

2.2. Diradical characters

In order to discuss the diradical characters and the spin densities, the LC-UBLYP/6-31G* method with a range separating parameter $\mu = 0.33$[32] was employed. Since the diradical character represents the instability of a chemical bond,[25–31] multiradical systems are characterized by multiple diradical characters (y_i) with non-zero values. In this study, the diradical character y_i [related to the highest occupied natural orbital (HONO) $- i$ and the lowest unoccupied natural orbital (LUNO) $+ i$, where $i = 0,1,\ldots$] is defined by the occupation numbers (n_k) of the natural orbitals (NOs) calculated using the LC-UBLYP/6-31G* method:

$$y_i = n_{\mathrm{LUNO}+i} = 2 - n_{\mathrm{HONO}-i} \qquad (1)$$

which takes a value ranging from 0 (closed-shell) to 1 (pure diradical). Unlike in UHF calculations, we do not evaluate spin projected diradical characters because the spin contamination effect is smaller in UDFT than in UHF. In fact, the diradical character is originally defined in the MC-SCF theory as twice the weight of the doubly-excited configuration in the singlet ground state but in spin-unrestricted single determinant schemes (like UHF and UDFT) it is formally expressed by eqn (1). The definitions and physical meaning of the diradical character have been discussed in several papers in connection with the *odd electron* number and density,[28–31] which are not observable but provide an index of chemical bond. These measures are useful for obtaining intuitive and pictorial descriptions of the open-shell characters and of their impact on various response properties.[31] Using eqn (1), the fractional occupation numbers in each pair of HONO $- i$ and LUNO $+ i$ provide the successive diradical characters, y_i, which also

represent the degree of correlation involved in the spin-unrestricted schemes.

2.3. Magnetic properties

The magnetic shielding tensors and magnetic susceptibility tensors calculations necessary to determine the magnetic properties were performed at the LC-UBLYP/6-31G* level using the GIAO method.[43] The NICS and $-\sigma_{zz}$ values are specifically calculated 1 Å above the molecular plane at positions corresponding to the centers of mass of the central and terminal rings, where a major contribution from π electrons is expected.[44] In addition, the three-dimensional ICSS[34] (for both the average and the out-of-plane components) were sketched using the PARAVIEW program.[45] Negative (positive) NICS and $-\sigma_{zz}$ values correspond to shielding (deshielding), and therefore negative (positive) NICS(1Å) and $-\sigma_{zz}$(1Å) values are associated, in first approximation, with aromatic (antiaromatic) rings.

2.4. Determination of γ

Our previous studies show that the LC-UBLYP method[32] can semi-quantitatively reproduce the γ values calculated using higher-order electron-correlated methods, *e.g.*, spin-unrestricted coupled cluster singles and doubles with a perturbative triples correction, for diradical molecules with intermediate and large diradical characters.[46] We therefore employed the LC-UBLYP method to calculate the longitudinal components of γ ($= \gamma_{xxxx}$), which is dominant in these one-dimensional systems. Following our previous studies,[17–19,21–23] the 6-31G* basis set was employed since it is known to be adequate for semi-quantitative comparisons of, at least, the longitudinal γ components of large diradical systems.

We applied the finite-field (FF) method[47] to calculate the static γ values. Within this approach, γ is calculated by carrying out a fourth-order numerical differentiation of the energy with respect to the applied external electric field. The field amplitudes were chosen to attain a numerical accuracy within an error of 1% on the γ value. All calculations were performed using the Gaussian 09[48] and 03[49] program packages.

3. Results and discussion

3.1. Size dependences of the diradical characters of DPAs and PAs

Table 1 lists the diradical characters y_i ($i = 0, 1$) of the singlet DPAs and PAs ($2 \leq N \leq 12$), while their size dependences are shown in Fig. 2. In DPAs, y_0 increases rapidly in the small N region ($N = 2$–6) and then saturates around $N = 10$. On the other hand, the PA systems are closed-shell for $N = 2$ to 4, and y_0 only starts emerging from $N = 5$ with smaller amplitudes than those of DPAs. On the other hand, the y_1 values of both systems are shown to emerge from intermediate N values ($N = 8$ for DPAs and 5 for PAs), indicating the appearance of a multi-radical (tetra-radical in this case) nature in both systems of large size.[42] In comparison with the PA case, where the y_0 and y_1 emerge from the same N ($= 5$), the y_0 of DPAs emerges from smaller N ($= 2$), while the y_1 of DPAs emerges from larger N ($= 8$). The origin of this feature is speculated as follows. As shown in previous studies,[41,42] small size PAs ($N < 6$) are closed-shell systems, while for $N \geq 6$ the odd electrons[28,30] appear on the zigzag edges, and the multi-radical nature also emerges with increasing size.[37,50,51] This explains the delayed increase in y_0 of PAs. On the other hand, the odd electrons of DPAs tend to be rather localized on the terminal five-membered rings, as supported by the increase of aromaticity in the central oligoacene region when increasing the DPA size. Therefore, the y_0 values of DPAs emerge faster than those of PAs, while their y_1 values, which are predicted to originate from the odd electrons on the zigzag edges of the six-membered rings, emerge for bigger systems ($N \geq 8$) than in the case of PAs ($N \geq 5$), though the increase rate of y_1 in DPAs is larger than in PAs.

In order to verify the above speculation, we investigate the spin density distributions of singlet DPAs and PAs from $N = 5$ to 9 (Fig. 3). Indeed, though spin polarization in the singlet state appears in the spin-unrestricted solutions and disappears in the spin-restricted solutions, it approximately represents the spatial features of odd electron density[28,30,31]

Table 1 Diradical characters (y_0 and y_1) for DPA and PA systems ($2 \leq N \leq 12$)[a] in their singlet states calculated from eqn (1)

	y_0		y_1	
N	DPA (singlet)	PA (singlet)	DPA (singlet)	PA (singlet)
2	0.212	0.000	0.002	0.000
3	0.393	0.000	0.007	0.000
4	0.602	0.000	0.012	0.000
5	0.744	0.118	0.015	0.016
6	0.836	0.330	0.018	0.054
7	0.895	0.541	0.021	0.105
8	0.929	0.666	0.146	0.159
9	0.947	0.745	0.305	0.219
10	0.956	0.800	0.485	0.285
11	0.961	0.839	0.609	0.356
12	0.965	0.867	0.690	0.426

[a] For DPA systems with D_{2h} symmetry ($2 \leq N \leq 12$), we have obtained spin unrestricted solutions at the LC-UBLYP/6-31G* level, which are the ground states while the spin-restricted ground state solutions have higher energies. Wavefunction stability was checked for all these compounds. PA systems with D_{2h} symmetry ($2 \leq N \leq 12$) have spin-unrestricted ground states except for $N = 2$–4, which display spin-restricted ground states.

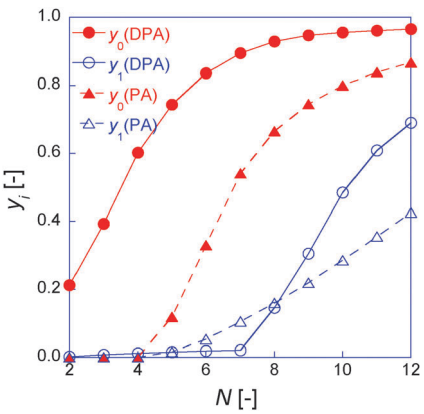

Fig. 2 Diradical characters (y_0 and y_1) *versus* N for singlet DPAs and PAs ($2 \leq N \leq 12$).

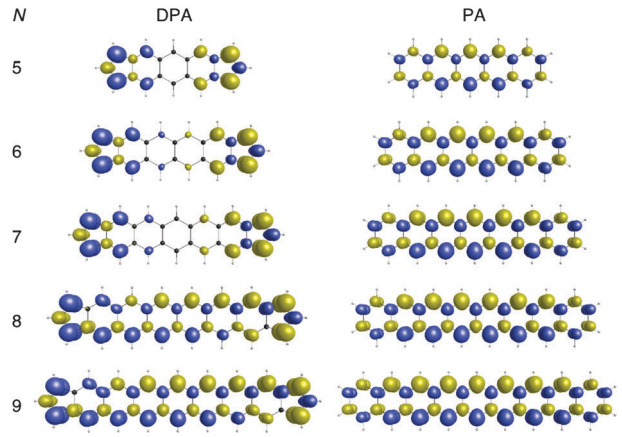

Fig. 3 Spin density distributions of DPAs and PAs in the singlet state calculated by the LC-(U)BLYP/6-31G* method ($5 \leq N \leq 9$). The yellow and blue surfaces represent α and β densities with iso-surfaces of ± 0.005 a.u., respectively.

and thereof of spin correlation. From these results, we observe that the spin polarizations in PAs (N = 5–9) and DPAs (N = 5–7) are characterized by transversal and longitudinal components, respectively, whereas in the case of large DPAs (N = 8–9) we observe both components. This behavior coincides with the size dependences of y_0 and y_1 in DPAs shown in Fig. 2 demonstrating that the increases in y_0 and y_1 correspond to the increases of spin polarizations in the longitudinal and transversal directions, respectively. Fig. 3 also exemplifies our prediction that the medium-size oligoacenes manifest spin polarizations in the transversal direction (odd electron distributions on both zigzag edges), the amplitudes of which gradually increase with size. Since open-shell singlet molecules with intermediate diradical characters are found to give enhanced γ values along the spin polarization direction,[17–23] the longitudinal γ of DPA is predicted to be enhanced in the intermediate y_0 region, which is associated with the longitudinal spin polarization, whereas the longitudinal γ of PA will not be affected by the increase in y_0, *i.e.*, the closed-shell feature is preserved in the longitudinal direction.

3.2. Relationship between aromaticity/antiaromaticity and diradical characters

Fig. 4 and Table 2 show the size dependences of NICS(1Å) and $-\sigma_{zz}$(1Å) values calculated on the central and terminal rings of singlet DPAs and PAs. In PAs, NICS(1Å) and $-\sigma_{zz}$(1Å) are all negative, suggesting an aromatic character (*on the basis of the shielding criteria of aromaticity*), which is also evident from the shielding topology maps presented in Fig. 5 that are similar to the benzene case, *i.e.*, one can observe a clear distinction between the shielding surface extending in the out-of-plane direction and the deshielding surface surrounding the molecular skeleton. Moreover, both NICS(1Å) and $-\sigma_{zz}$(1Å) amplitudes related to the central ring decrease with N whereas those on the terminal rings of PAs are almost independent of N, so that the former become smaller than the latter for $N \geq 7$. This size dependence of the shielding properties on the central rings of PAs is associated with the spin polarization on the zigzag edges, which is larger than that

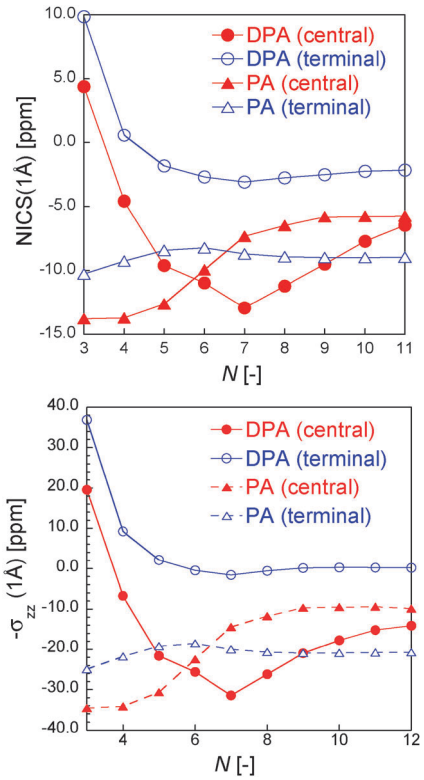

Fig. 4 Size dependences of NICS(1Å) (top) and $-\sigma_{zz}$(1Å) (bottom) values on the central and terminal rings of DPA and PA in their singlet state calculated by the LC-(U)BLYP/6-31G* method. Positive and negative values indicate deshielded and shielded positions, respectively, to be related to the spatial shielding maps presented in Fig. 5.

in the terminal region and which increases with N (Fig. 3), in parallel with y_0 and y_1. Moreover, from the $\Delta\chi/N$ values presented in Table 2 and Fig. 6, we have a clear indication, *on the basis of the magnetic susceptibility criterion of aromaticity*, that the global aromatic nature of these compounds is strictly decreasing as a function of their size, meaning that the increase in the diradical character of PAs can be associated with the decrease in the degree of aromaticity as increasing N. These tendencies coincide with previous results,[52] though *closed-shell solutions* were used to examine the aromaticity in contrast to our study. Note that in terms of local aromaticity, our investigation of the shielding criteria of aromaticity applied to PAs is in perfect agreement with the energetic data presented in ref. 51 *i.e.*, for big systems ($N > 7$) "the central rings exhibit less local aromaticity than the edge rings".

Next, we examined the size dependences of the shielding properties of DPAs (Fig. 4), which are significantly different from those of PAs. So, the central ring regions always sustain a more diamagnetic effect of the induced currents than the terminal ones, which could be rationalized according to the Hückel rule by the fact that the central rings are six-membered rings while the terminal rings are constituted by only 5 atoms, meaning that the most intense diatropic currents tend to be located around the phenyl rings. In the specific case of *s*-indacene [DPA(N = 3)], the $\Delta\chi$ value (Fig. 6) and the shielding topology around both the central and terminal rings (Fig. 5), which is very similar to the case of the cyclobutadiene molecule

Table 2 NICS(1Å) and $-\sigma_{zz}$(1Å) values (on the central and terminal rings) as well as magnetic susceptibility anisotropy, $\Delta\chi$, (a.u.) for DPA and PA systems ($2 \leq N \leq 12$) in their singlet states

	NICS(1Å) (central)		NICS(1Å) (terminal)		$-\sigma_{zz}$(1Å) (central)		$-\sigma_{zz}$(1Å) (terminal)		$\Delta\chi/N$	
N	DPA	PA	DPA	PA	DPA	PA	DPA	PA	DPA	PA
2	—	—	109.63	−11.46	—	—	335.25	−28.56	48.47	−13.29
3	4.40	−13.79	9.85	−10.28	19.57	−34.57	36.86	−24.90	−0.15	−13.29
4	−4.57	−13.72	0.59	−9.27	−6.71	−34.16	9.27	−21.78	−5.88	−13.36
5	−9.62	−12.63	−1.82	−8.43	−21.60	−30.66	2.16	−19.21	−7.96	−12.63
6	−10.98	−9.96	−2.70	−8.22	−25.61	−22.47	−0.43	−18.55	−9.07	−11.60
7	−12.94	−7.33	−3.09	−8.70	−31.43	−14.43	−1.57	−20.00	−9.80	−10.91
8	−11.22	−6.47	−2.76	−8.93	−26.20	−11.75	−0.55	−20.68	−9.56	−10.59
9	−9.51	−5.79	−2.52	−9.00	−20.96	−9.64	0.16	−20.89	−9.23	−10.39
10	−7.71	−5.76	−2.25	−9.00	−15.45	−9.53	0.97	−20.88	−8.98	−10.24
11	−6.46	−5.72	−2.16	−8.97	−11.65	−9.39	1.25	−20.80	−8.89	−10.12
12	−6.13	−5.89	−2.16	−8.95	−10.63	−9.88	1.24	−20.73	−8.88	−10.00

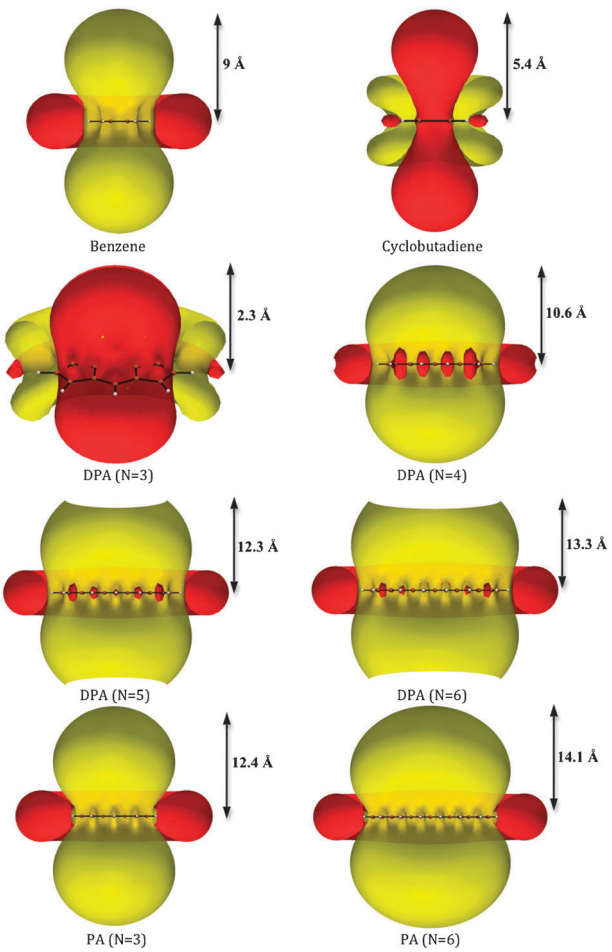

Fig. 5 Evolution of the shielding topology in small DPAs, represented by $-\sigma_{zz}$ ICSS maps corresponding to ±0.4 ppm isocontours. Shielding surfaces (corresponding to negative values) are represented in yellow, and deshielding surfaces (positive values) are represented in red. Note that the global topology for bigger DPAs ($N > 6$) is similar to the case $N = 6$, *i.e.* we can observe a pair of extended shielding/deshielding surfaces and shielding transition zones around the two pairs of terminal cycles. These topologies are compared to those of two selected polyacenes ($N = 3, 6$), which present the out-of-plane shielding topology of the whole polyacene series. Those of benzene and cyclobutadiene are also sketched as references since they correspond to the model aromatic and antiaromatic systems, respectively.

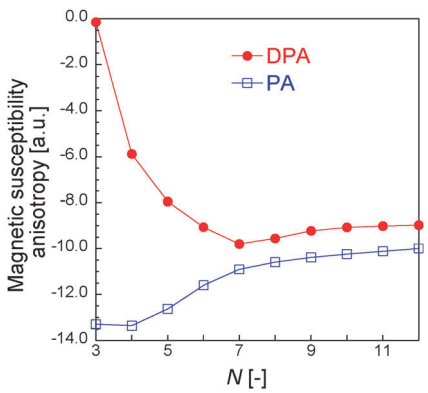

Fig. 6 Size dependences of the magnetic susceptibility anisotropy (a.u.) of DPAs and PAs in their singlet state calculated by the LC-(U)BLYP/6-31G* method.

also presented in Fig. 5,[53] all indicate a clear antiaromatic nature of this system.[34–36,44] On the other hand, considering the $\Delta\chi$ values and the shielding topologies, larger DPAs present typical magnetic responses of globally aromatic systems. Note that the positive $-\sigma_{zz}$(1Å) values associated with the terminal rings in the DPAs ($N = 4$–5) (Table 2) are not to be necessarily related to a local antiaromatic character. Indeed, one can see from Fig. 5 that in these cases the chosen shielding probes are in fact positioned inside "spatially localized" shielding transition zones centered around the terminal cycles centers, *i.e.*, where a local transition from deshielding to shielding surfaces occurs, while the whole molecular domain is still surrounded by large shielding/deshielding pairs that are often associated with global diatropic (aromatic) behaviors.[34,35] The presence of such shielding transition zones may however seem confusing when considering this kind of behaviour, but can be understood by referring to previous investigations of the magnetically induced currents in the *closed-shell forms* of *s*-indacene and other DPAs:[54–56] when increasing the size of the systems from pentalene to large DPAs, a reversal of the induced π currents from paratropic to diatropic occurs, which is mainly explained by the decrease of the paratropic current contributions (based on HOMO–LUMO gap arguments[56]) as well as by the increase of diatropic contributions (mainly concentrated on the inner phenyl rings). Based on energetic and magnetic arguments, it has been shown that due to the increase of the diradical character of

DPAs with their size, these systems tend to behave more and more like PAs, which is still consistent with some of our results on open-shell forms, *i.e.*, the emergence of a global aromatic character, and the persistence of shielding transition zones, mainly localized at the centers of the terminal rings for the biggest systems, because of the main concentration of the strong π diatropic zones around the inner rings. Consistently, results presented in ref. 57 on cyclopropane show that apparitions of shielding transition zones originate from the competitions between the distinct paramagnetic/diamagnetic influences of the induced π and σ currents, as can be seen, for example, in the cases of 6-cycle PA and DPA molecules for which the π and σ induced currents have been calculated[58] (Fig. 7). Note the diatropic π currents occurring in the DPA molecule, as well as the difference of maximal intensity of these currents with respect to the PA case. Then, on the basis of the current density maps presented in ref. 54 and 55, we can propose the following conclusions: (i) pentalene ($N = 2$) and *s*-indacene ($N = 3$) have a strong π paratropic character, making their antiaromatic-like properties easy to understand[59] (note however that such parallel between π currents and antiaromatic-like properties is not straightforward, as *e.g.* in the case of *s*-indacene for which a detailed study[54] has shown that the competition between the σ and π currents is complex, as the strong delocalized π paratropic current seems to be "enhanced" by σ paratropic currents in the inner-cycle region, while being compensated by some σ diatropic flow in the outer region of the molecular domain, resulting in a weak diatropic circulation surrounding a region of quite stronger paratropic currents around the molecular cycles, see Fig. 3 of ref. 54. So, the paramagnetic effect of the currents on the properties is not to be attributed to the only π system.); (ii) the case of the DPA ($N = 4$) system is the most complex of the series, as it presents a small π paratropic character that however does not seem strong enough to counterbalance all the effects of the peripheral diatropic σ current, as can be seen in Fig. 2 of ref. 55. This results in the manifestation of local paratropic currents inside each cycle of this system and of a less intense but more delocalized diatropic current all around the molecular skeleton, which explains the apparition of shielding transition zones at each ring center due to their competition, in contrast to the large aromatic-like shielding surface that we can attribute mostly to the delocalized diatropic current; and then (iii) the bigger DPAs ($N > 4$) exhibit π diatropic currents of increasing intensity, which counterbalance more the paramagnetic effects of the σ currents, especially at the level of the inner phenyl cycles because of the "concentration" of the π currents we explained hereinabove.

Note however that while it is easy to suggest the possible origins of the magnetic properties in terms of induced currents, we still lack tools to simulate in a consistent way the currents induced in the *open-shell states* of the DPA and PA systems in order to assess completely the correlation between the shielding and susceptibility criteria and the aromatic nature of these systems.

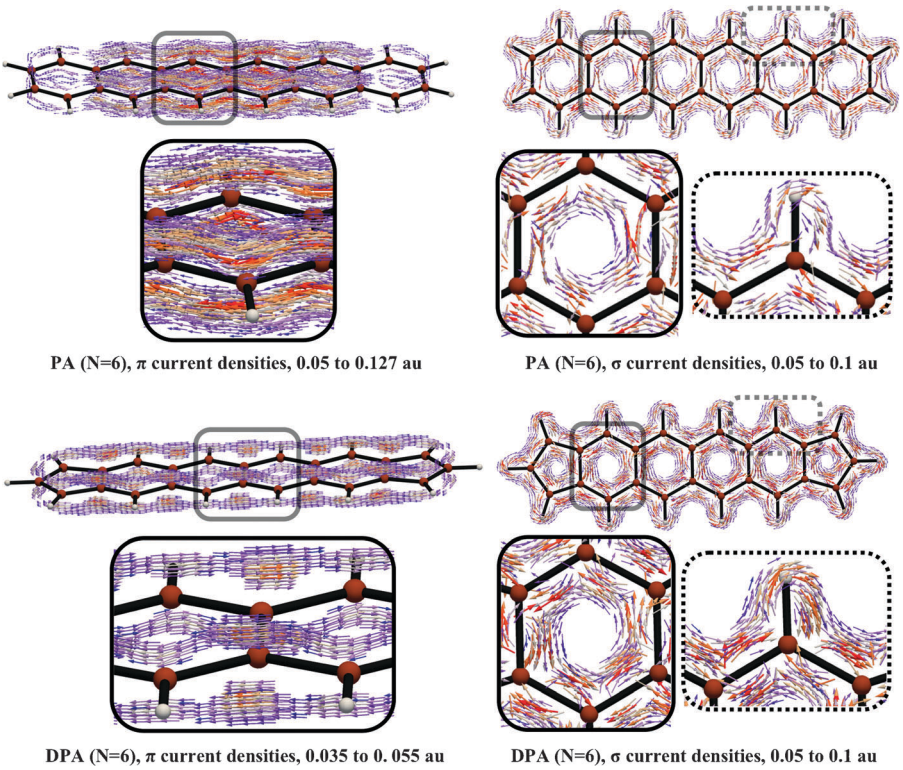

Fig. 7 Current density maps calculated on the closed-shell structures of $N = 6$ PA (top) and DPA (bottom) molecules under a magnetic field ($\boldsymbol{B}_z$) directed perpendicular to the molecular plane. The color code (blue to red) corresponds to a variation of the modulus of the current density between the extrema (minimum to maximum) within the range indicated below each map. For each map, the reported maximal value of the π current range corresponds to the maximal value of all the π currents around the molecule. Clockwise (*anticlockwise*) circulation of the current density denotes a diatropic (*paratropic*) current.

On the basis of the Hückel rule, in *s*-indacene the π-electrons seem little delocalized from the central six-membered ring to the two terminal five-membered rings, while in the case of DPAs with more than two six-membered rings we can expect a larger π-electron delocalization from the 6-membered to the 5-membered rings. Indeed, the terminal rings of DPAs with $N > 3$ exhibit slight- or non-aromatic character, while the shielding criteria associated with the terminal rings of DPAs become almost constant for $N \geq 5$, similarly to the case of PAs. In the cases of the biggest DPA systems for which we have observed the emergence of a multiradicalar character ($N \geq 7$), we have to note that $\Delta\chi$ and the shielding properties around the central and terminal rings are decreasing in absolute value, indicating a decrease in local and global aromaticity, which is predicted to originate from the spin polarization appearing on the zigzag edges in the middle PA region [see Fig. 3 and 4 for PAs and DPAs ($N \geq 7$)].

As a result, for DPAs, the increase of y_0 with size can be related to the slight- or non-aromaticity on the terminal five-membered rings, while the appearance and increase of y_1 after $N = 7$ is related to the decrease of aromaticity in the central ring region. On the other hand, in the case of PAs, the increases of y_0 and y_1 with N, corresponding to the appearance and increase of spin polarization on the zigzag edges in the intermediate N region, can be associated with the decrease of the global aromatic character.

3.3. Size dependences of the longitudinal γ in relation to the diradical characters

Fig. 8(a) and Table 3 show the size dependences of the longitudinal γ/N (γ values per fused-ring) for singlet DPAs and PAs as well as for triplet DPA systems. The geometries optimized for singlet DPAs were employed for calculating the γ of triplet DPAs to highlight the effects of spin state multiplicity.

The γ/N of singlet PAs, having negligible spin polarization in the longitudinal direction, displays a monotonic increase with N, which is caused by the increase of the π-conjugation length.[36] In contrast, the γ/N of singlet DPAs exhibits a unique behavior characterized by a stronger size dependence, larger amplitudes in comparison to singlet PA systems up to $N = 7$, and presenting a hump around $N = 8$. For larger systems ($N > 8$), the size dependence of γ/N in DPAs gets more similar to the case of singlet PAs. Since for each N, the π-conjugation lengths are similar in PA and DPA systems, this difference of behavior can be attributed to the intermediate diradical characters y_0 of singlet DPAs (0.212–0.895 for $N = 2$–7). As shown in Fig. 8(a), the increase rate of γ/N for singlet DPAs reduces from $N = 7$ and even γ/N temporarily decreases at $N = 9$. This local decrease is expected from the y_0 value coming close to 1. On the other hand, the appearance and the increase of y_1 (corresponding to the transversal spin polarization) after $N = 7$ for singlet DPA do not contribute to the enhancement of the longitudinal γ. Fig. 8(b) shows the size dependence of the γ enhancement ratio [γ(singlet DPA)/γ(singlet PA)], which attains a maximum around $N = 4$, since it corresponds to the intermediate diradical character region ($y_0 \approx 0.6$) for singlet DPA.

A further assessment of the effect of diradical characters of singlet DPAs consists in examining the γ/N values of triplet

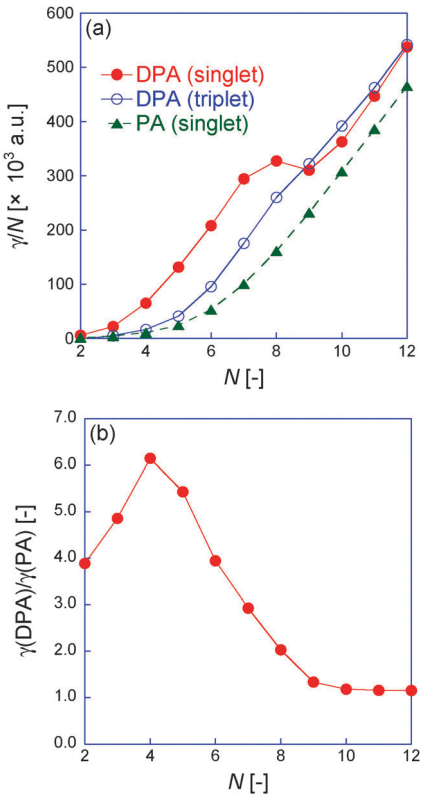

Fig. 8 Size dependences of γ values per fused-ring unit of DPAs and PAs in the singlet state and of DPA in the triplet state (a) and size dependences of the γ enhancement ratio, *i.e.*, γ(singlet DPA)/γ(singlet PA) (b). The γ values are calculated by the LC-(U)BLYP/6-31G* method.

Table 3 LC-(U)BLYP/6-31G* longitudinal second hyperpolarizabilities per fused ring (γ/N) [in 10^5 a.u.] for DPA systems ($2 \leq N \leq 12$) in their singlet and triplet states in comparison to those of PA systems in their singlet state

	γ/N		
N	DPA (singlet)	DPA (triplet)	PA (singlet)
2	5.5	−1.03	1.42
3	21.7	5.11	4.47
4	65.0	16.1	10.6
5	131	41.0	24.2
6	208	95.3	52.8
7	294	176	100
8	328	260	161
9	310	322	232
10	363	392	308
11	447	463	386
12	538	542	466

DPAs, which are regarded as pure open-shell systems. As seen from Fig. 8(a), the γ/N of triplet DPAs differs from that of singlet DPAs only in the huge increase of γ/N values for singlet DPAs up to $N = 7$–8. Indeed, for $N \geq 9$, the γ values of the singlet and triplet DPAs are similar to each other since $y_0 \approx 1$. Judging from these variations in γ of singlet and triplet DPAs as well as the variation in y_0 of singlet DPAs, the excess increase for small singlet DPAs ($N \leq 8$) is caused by the intermediate diradical character y_0. It is also noted that a constant difference in γ/N between singlet DPA and PA

systems for each N value is still observed for $N \geq 9$. This difference is probably due to the spin polarization between the terminal rings (see $N = 9$ in Fig. 3).

4. Concluding remarks

Theoretical LC-BLYP calculations have shown that γ of singlet DPAs is significantly enhanced with increasing system size. This behavior, which is associated with an increase in the longitudinal spin polarization between the terminal five-membered rings, is consistent with previous studies[17–23] where γ is maximized for intermediate diradical character (y_0). The size dependence of the diradical character is also found to cause a hump in the γ/N evolution for singlet DPA around $N = 8$. Therefore, for $N \leq 9$, the γ/N values of singlet DPAs and PAs are significantly different though the number of carbon atoms is almost identical. In the case of singlet PAs, the diradical characters y_0 and y_1, the various magnetic properties and the γ/N values vary monotonically with N. On the other hand, for singlet DPAs, the shielding, the magnetizability, and γ/N values exhibit extrema near $N = 8$ due to the appearance of transversal spin polarization in the middle six-membered rings in addition to the longitudinal spin polarization between the terminal five-membered rings.

Moreover, it is shown that for singlet DPAs the longitudinal spin polarization (characterized by y_0) is associated with the antiaromaticity ($N \leq 3$) and the slight- or non-aromaticity ($N \geq 4$) in the terminal five-membered rings, whereas the appearance of transversal spin-polarization (characterized by y_1) is associated with the decrease in the aromaticity in the inner six-membered rings as shown for large PAs.[52] This is also exemplified by the fact that the difference in γ values between singlet PA and DPA systems becomes small for large systems ($N \geq 9$) because the contribution of spin polarization in the middle six-membered rings becomes dominant as N increases. In conclusion, the exceptional behaviors in singlet DPAs for small N ($N < 9$) are caused by the increase in diradical character y_0 correlated with the anti-aromaticity or the slight-/non-aromaticity of terminal rings and the corresponding emergence of a global aromatic character. Such a relationship between aromaticity/antiaromaticity and diradical character is useful for designing real open-shell NLO molecules through the control of diradical characters. To our knowledge, this is the first time such relationships between electronic, magnetic, and nonlinear optical properties are drawn for organic compounds.

Acknowledgements

This work was supported by Grant-in-Aid for Scientific Research (Nos. 21350011 and 20655003) and "Japan–Belgium Cooperative Program" (J091102006) from Japan Society for the Promotion of Science (JSPS), and the global COE (center of excellence) program "Global Education and Research Center for Bio-Environmental Chemistry" of Osaka University. Theoretical calculations were partly performed at the Research Center for Computational Science (Okazaki, Japan) and at the Interuniversity Scientific Computing Facility (ISCF) installed at the Facultés Universitaires Notre-Dame de la Paix (FUNDP, Namur, Belgium), for which financial support from the FRS-FRFC (Convention No. 2.4.617.07.F) and the FUNDP is acknowledged. R.C. thanks the F.R.S.-FNRS for his research fellow position. This work has also been supported by the Academy Louvain (ARC "Extended π-Conjugated Molecular Tinkertoys for Optoelectronics, and Spintronics") and by the Belgian Government IUAP No P06-27 "Functional Supramolecular Systems".

References

1 *Stable Radicals – Fundamentals and Applied Aspects of Odd-Electron Compounds*, ed. R. G. Hicks, John Wiley & Sons, Chichester, 2010.
2 K. S. Novoselov, A. K. Geim, S. V. Morozov, D. Jiang, Y. Zhang, S. V. Dubonos, V. Grigorieva and A. A. Firsov, *Science*, 2004, **306**, 666.
3 A. H. Castro Neto, F. Guinea, N. M. R. Peres, K. S. Novoselov and A. K. Geim, *Rev. Mod. Phys.*, 2009, **81**, 109.
4 S. Dutta and S. K. Pati, *J. Mater. Chem.*, 2010, **20**, 8207.
5 L. J. Zhi and K. Müllen, *J. Mater. Chem.*, 2008, **18**, 1472.
6 C. Tönshoff and H. F. Bettinger, *Angew. Chem., Int. Ed.*, 2010, **49**, 4125.
7 A. Konishi, Y. Hirao, M. Nakano, A. Shimizu, E. Botek, B. Champagne, D. Shiomi, K. Sato, T. Takui, K. Matsumoto, H. Kurata and T. Kubo, *J. Am. Chem. Soc.*, 2010, **132**, 11021.
8 S. Di Motta, F. Negri, D. Fazzi, C. Castiglioni and E. V. Canesi, *J. Phys. Chem. Lett.*, 2010, **1**, 3334.
9 R. Ponce Ortiz, J. Casado, S. R. Gonzalez, V. Hernandez, J. T. Lopez Navarrete, P. M. Viruela, E. Orti, K. Takimya and T. Otsubo, *Chem.–Eur. J.*, 2010, **16**, 470.
10 P. J. Boratynski, M. Pink, S. Rajca and A. Rajca, *Angew. Chem., Int. Ed.*, 2010, **49**, 5459.
11 G. Trinquier, N. Suaud and J. P. Malrieu, *Chem.–Eur. J.*, 2010, **16**, 8762.
12 I. Paci, J. C. Jonhson, X. Chen, G. Rana, D. Popovic, D. E. David, A. J. Nozik, M. A. Ratner and J. Michl, *J. Am. Chem. Soc.*, 2006, **128**, 16546.
13 A. Shimizu, M. Uruichi, K. Yakushi, H. Matsuzaki, H. Okamoto, M. Nakano, Y. Hirao, K. Matsumoto, H. Kurata and T. Kubo, *Angew. Chem., Int. Ed.*, 2009, **48**, 5482.
14 Y. H. Tian and M. Kertesz, *J. Am. Chem. Soc.*, 2010, **132**, 10648.
15 P. Bag, M. E. Itkis, S. K. Pal, B. Donnadieu, F. S. Tham, H. Park, J. A. Schlueter, T. Siegrist and R. C. Haddon, *J. Am. Chem. Soc.*, 2010, **132**, 2684.
16 K. Kamada, K. Ohta, T. Kubo, A. Shimizu, Y. Morita, K. Nakasuji, R. Kishi, S. Ohta, S. Furukawa, H. Takahashi and M. Nakano, *Angew. Chem., Int. Ed.*, 2007, **46**, 3544.
17 M. Nakano, R. Kishi, T. Nitta, T. Kubo, K. Nakasuji, K. Kamada, K. Ohta, B. Champagne, E. Botek and K. Yamaguchi, *J. Phys. Chem. A*, 2005, **109**, 885.
18 M. Nakano, R. Kishi, S. Ohta, A. Takebe, H. Takahashi, S.-I. Furukawa, T. Kubo, Y. Morita, K. Nakasuji, K. Yamaguchi, K. Kamada, K. Ohta, B. Champagne and E. Botek, *J. Chem. Phys.*, 2006, **125**, 074113.
19 M. Nakano, T. Kubo, K. Kamada, K. Ohta, R. Kishi, S. Ohta, N. Nakagawa, H. Takahashi, S. Furukawa, Y. Morita, K. Nakasuji and K. Yamaguchi, *Chem. Phys. Lett.*, 2006, **418**, 142.
20 M. Nakano, R. Kishi, S. Ohta, H. Takahashi, T. Kubo, K. Kamada, K. Ohta, E. Botek and B. Champagne, *Phys. Rev. Lett.*, 2007, **99**, 033001.
21 M. Nakano, H. Nagai, H. Fukui, K. Yoneda, R. Kishi, H. Takahashi, A. Shimizu, T. Kubo, K. Kamada, K. Ohta, B. Champagne and E. Botek, *Chem. Phys. Lett.*, 2008, **467**, 120.
22 H. Nagai, M. Nakano, K. Yoneda, H. Fukui, T. Minami, S. Bonness, R. Kishi, H. Takahashi, T. Kubo, K. Kamada, K. Ohta, B. Champagne and E. Botek, *Chem. Phys. Lett.*, 2009, **477**, 355.
23 K. Yoneda, M. Nakano, R. Kishi, H. Takahashi, A. Shimizu, T. Kubo, K. Kamada, K. Ohta, B. Champagne and E. Botek, *Chem. Phys. Lett.*, 2009, **480**, 278.
24 M. Kertesz, C. H. Choi and S. Yang, *Chem. Rev.*, 2005, **105**, 3448.

25 K. Yamaguchi, in *Self-Consistent Field: Theory and Applications*, ed. R. Carbo and M. Klobukowski, Elsevier, Amsterdam, 1990, p. 727.
26 S. Yamanaka, M. Okumura, M. Nakano and K. Yamaguchi, *J. Mol. Struct.*, 1994, **310**, 205.
27 E. F. Hayes and A. K. Q. Siu, *J. Am. Chem. Soc.*, 1971, **93**, 2090.
28 K. Takatsuka, T. Fueno and K. Yamaguchi, *Theor. Chim. Acta*, 1978, **48**, 175.
29 V. N. Staroverov and E. Davidson, *Chem. Phys. Lett.*, 2000, **330**, 161.
30 M. Head-Gordon, *Chem. Phys. Lett.*, 2003, **372**, 508.
31 M. Nakano, H. Fukui, T. Minami, K. Yoneda, Y. Shigeta, R. Kishi, B. Champagne, E. Botek, T. Kubo, K. Ohta and K. Kamada, *Theor. Chem. Acc.*, 2011, DOI: 10.1007/s00214-010-0871-y.
32 H. Iikura, T. Tsuneda, T. Yanai and K. Hirao, *J. Chem. Phys.*, 2001, **115**, 3540.
33 P. v. R. Schleyer, C. Maerker, A. Dransfield, H. Jiao and N. J. R. v. E. Hommes, *J. Am. Chem. Soc.*, 1996, **118**, 6317.
34 S. Klod and E. Kleinpeter, *J. Chem. Soc., Perkin Trans. 2*, 2001, 1893.
35 Z. Chen, C. Wannere, C. Corminboeuf, R. Puchta and P. v. R. Schleyer, *Chem. Rev.*, 2005, **105**, 3842.
36 P. Lazzeretti, *Phys. Chem. Chem. Phys.*, 2004, **6**, 217.
37 T. Bally, S. Chai, M. Neuenschwander and Z. Zhu, *J. Am. Chem. Soc.*, 1997, **119**, 1869.
38 J. D. Dunitz, C. Kruger, H. Irngartinger, E. F. Maverick, Y. Wang and M. Nixdorf, *Angew. Chem., Int. Ed. Engl.*, 1988, **27**, 3.
39 R. H. Hertwig, M. C. Holthausen, W. Koch and Z. B. Maksic, *Angew. Chem., Int. Ed. Engl.*, 1994, **33**, 1192.
40 Note that this qualification of "slight effect" is not true regarding the absolute values of $\Delta\chi$, but qualitatively it has no impact on the overall evolution of $\Delta\chi/N$ as a function of N: for *s*-indacene, $\Delta\chi/N(D_{2h}) = -0.1$ a.u. *vs.* $\Delta\chi/N(C_{2h}) = 3.1$ a.u. (at the LC-UBLYP/6-31G*//UB3LYP/6-311G* level of approximation).
41 M. Bendikov, H. M. Düong, K. Starkey, K. N. Houk, E. A. Carter and F. Wudl, *J. Am. Chem. Soc.*, 2004, **126**, 7416.
42 H. Nagai, M. Nakano, K. Yoneda, R. Kishi, H. Takahashi, A. Shimizu, T. Kubo, K. Kamada, K. Ohta, E. Botek and B. Champagne, *Chem. Phys. Lett.*, 2010, **489**, 212.
43 K. Ruud, T. Helgaker, K. L. Bak, P. Jørgensen and H. J. A. Jensen, *J. Chem. Phys.*, 1993, **99**, 3847.
44 P. v. R. Schleyer and H. Jiao, *Pure Appl. Chem.*, 1996, **68**, 209.
45 Paraview 3.4.0, Sandia Corporation, Kitware Inc., 2005–2008.
46 R. Kishi, S. Bonness, K. Yonda, H. Takahashi, M. Nakano, E. Botek, B. Champagne, T. Kubo, K. Kamada, K. Ohta and T. Tsuneda, *J. Chem. Phys.*, 2010, **132**, 094107.
47 H. D. Cohen and C. C. J. Roothaan, *J. Chem. Phys.*, 1965, **43**, S34.
48 M. J. Frisch, G. W. Trucks, H. B. Schlegel, G. E. Scuseria, M. A. Robb, J. R. Cheeseman, G. Scalmani, V. Barone, B. Mennucci, G. A. Petersson, H. Nakatsuji, M. Caricato, X. Li, H. P. Hratchian, A. F. Izmaylov, J. Bloino, G. Zheng, J. L. Sonnenberg, M. Hada, M. Ehara, K. Toyota, R. Fukuda, J. Hasegawa, M. Ishida, T. Nakajima, Y. Honda, O. Kitao, H. Nakai, T. Vreven, J. A. Montgomery, Jr., J. E. Peralta, F. Ogliaro, M. Bearpark, J. J. Heyd, E. Brothers, K. N. Kudin, V. N. Staroverov, R. Kobayashi, J. Normand, K. Raghavachari, A. Rendell, J. C. Burant, S. S. Iyengar, J. Tomasi, M. Cossi, N. Rega, J. M. Millam, M. Klene, J. E. Knox, J. B. Cross, V. Bakken, C. Adamo, J. Jaramillo, R. Gomperts, R. E. Stratmann, O. Yazyev, A. J. Austin, R. Cammi, C. Pomelli, J. W. Ochterski, R. L. Martin, K. Morokuma, V. G. Zakrzewski, G. A. Voth, P. Salvador, J. J. Dannenberg, S. Dapprich, A. D. Daniels, Ö. Farkas, J. B. Foresman, J. V. Ortiz, J. Cioslowski and D. J. Fox, *GAUSSIAN09 (Revision A.02)*, Gaussian, Inc., Wallingford, CT, 2009.
49 M. J. Frisch, G. W. Trucks, H. B. Schlegel, G. E. Scuseria, M. A. Robb, J. R. Cheeseman, J. A. Montgomery Jr., T. Vreven, K. N. Kudin, J. C. Burant, J. M. Millam, S. S. Iyengar, J. Tomasi, V. Barone, B. Mennucci, M. Cossi, G. Scalmani, N. Rega, G. A. Petersson, H. Nakatsuji, M. Hada, M. Ehara, K. Toyota, R. Fukuda, J. Hasegawa, M. Ishida, T. Nakajima, Y. Honda, O. Kitao, H. Nakai, M. Klene, X. Li, J. E. Knox, H. P. Hratchian, J. B. Cross, C. Adamo, J. Jaramillo, R. Gomperts, R. E. Stratmann, O. Yazyev, A. J. Austin, R. Cammi, C. Pomelli, J. W. Ochterski, P. Y. Ayala, K. Morokuma, G. A. Voth, P. Salvador, J. J. Dannenberg, V. G. Zakrzewski, S. Dapprich, A. D. Daniels, M. C. Strain, O. Farkas, D. K. Malick, A. D. Rabuck, K. Raghavachari, J. B. Foresman, J. V. Ortiz, Q. Cui, A. G. Baboul, S. Clifford, J. Cioslowski, B. B. Stefanov, G. Liu, A. Liashenko, P. Piskorz, I. Komaromi, R. L. Martin, D. J. Fox, T. Keith, M. A. Al-Laham, C. Y. Peng, A. Nanayakkara, M. Challacombe, P. M. W. Gill, B. Johnson, W. Chen, M. W. Wong, C. Gonzalez and J. A. Pople, *GAUSSIAN 03 (Revision C.02)*, Gaussian, Inc., Wallingford, CT, 2004.
50 J. Hachmann, J. J. Dorando, M. Avilés and G. K. L. Chan, *J. Chem. Phys.*, 2007, **127**, 134309.
51 D. Jiang and S. Dai, *J. Phys. Chem. A*, 2008, **112**, 332.
52 J. Aihara and H. Kanno, *J. Phys. Chem. A*, 2005, **109**, 3717. However their NICS evolution is not identical to ours, because their NICS at the central rings are always more negative than the NICS at the terminal ones, due to differences in the methodological approaches.
53 Y.-M. Legrand, A. van der Lee and M. Barboiu, *Science*, 2010, **329**, 299. The cyclobutadiene geometry used for the shielding calculations presented in Fig. 5 corresponds to the rectangular geometry described in this reference, for which the two methyl substituents have been replaced by two hydrogen atoms. A relaxation of the C–H bonds has been carried out afterwards.
54 R. Soriano Jartin, A. Ligabue, A. Soncini and P. Lazzeretti, *J. Phys. Chem. A*, 2002, **106**, 11806–11814.
55 R. Havenith, J. Engelberts, P. W. Fowler, E. Steiner, J. van Lenthe and P. Lazzeretti, *Phys. Chem. Chem. Phys.*, 2004, **6**, 289.
56 M. Makino and J. Aihara, *Phys. Chem. Chem. Phys.*, 2008, **10**, 591.
57 R. Carion, B. Champagne, G. Monaco, R. Zanasi, D. Bonifazi, S. Pelloni and P. Lazzeretti, *J. Chem. Theory Comput.*, 2010, **6**, 2002.
58 These current density maps have been calculated at the CHF/6-31G** level of theory (using the RB3LYP/6-311G* optimized structures) *via* the CTOCD-DZ2 procedure implemented in the SYSMO package: (*a*) P. Lazzeretti, M. Malagoli, R. Zanasi, Technical Report on Project "Sistemi Informatici e Calcolo Parallelo"; Research Report 1/67, CNR, 1991; (*b*) R. Zanasi, *J. Chem. Phys.*, 1996, **105**, 1460–1469. More details on the computational procedure can also be found in ref. 57.
59 Note that in the case of the pentalene molecule the amplitudes of the antiaromatic-like magnetic properties are ridiculously huge due to our choice of considering all the systems under the constraint of D_{2h} symmetry. Indeed, for comparison the diradical characters and magnetic properties of this system in the C_{2h} symmetry, *i.e.*, its fully relaxed structure, evaluated at the LC-UBLYP/6–31G* level of theory are: $y_0 = 0.000$, $y_1 = 0.000$, NICS(1Å) = 15.12 ppm, $-\sigma_{zz}$(1Å) = 52.24 ppm, $\Delta\chi/N = 3.58$ ppm. However, it has already been justified that even if these results differ greatly in absolute value, it has no significant effect on the global size dependence of the properties of DPAs.